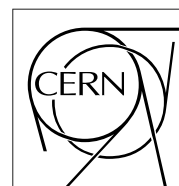


The Compact Muon Solenoid Experiment

CMS Note

Mailing address: CMS CERN, CH-1211 GENEVA 23, Switzerland



November 1, 1999

Muon Track Matching

A. Benvenuti¹⁾, D. Denegri²⁾, V. Genchev³⁾, A. Khanov⁴⁾, N. Stepanov⁴⁾, P. Vankov³⁾

Abstract

For most physical processes the tracks observed in the muon stations must be matched with the corresponding tracks in the inner tracker, the external muon system providing muon identification and triggering but the tracker points giving the precise momentum measurement at lower momenta. For high momenta the momentum resolution is much improved by the interconnection of inner and outer measurements. The matching of outer and inner measurements is more delicate in case of muons embedded in jets. A study of the matching procedure was carried out using samples of $b\bar{b}$ jets at high P_t , requiring $b\bar{b} \rightarrow \mu$ decays.

¹⁾ INFN, Bologna, Italy

²⁾ DAPNIA, Saclay, France

³⁾ INRNE, Sofia, Bulgaria

⁴⁾ ITEP, Moscow, Russia

1 Motivation

Identification and measurement of muons in the inner tracker using its high spatial resolution and excellent momentum measurement in the 4T field is a very important and demanding task, particularly for muons in jets. In the muon system the occupancy is low and pattern recognition is relatively easy, provided the particle reaches the muon system at all, which is the case for the barrel is $P_t^\mu \gtrsim 4$ GeV. For non-isolated muons the main difficulty is to match the track observed in the muon stations with the correct candidate in the inner tracker in case of the high track density inside a jet. These situations arise for example in muon tagging of b -jets, in $b \rightarrow J/\psi(\rightarrow \mu\mu) + X$ cascades in b and top physics, in SUSY(\tilde{q}, \tilde{g}) physics and most dramatically in very high E_t (TeV scale) jets such as heavy flavour (b, c) QCD jets giving rise to "muon bundles" within jets.

The matching strategy is based on the use of the full parameter space, i.e. on both the reconstructed momentum and the position in a given plane for the two tracks, one in the muon system and the other in the inner tracker. The quantities monitored are the efficiency of matching (number of muons matched over number of muons reconstructed), the muon matching impurity (1 - number of muons matched over number of tracks matched) and generation of "ghost" and "fake" tracks.

2 CMS model and data sample

The results discussed here are obtained using a detailed GEANT description of the complete CMS detector of TDR design. In all simulations the effects of the 4T field are fully included.

We have performed a GEANT simulation of the response to $b\bar{b}$ jets with transverse momenta P_t^{jet} of 50, 100 and 200 GeV (which corresponds to the P_t range of b -jets in $t\bar{t}$ production) and at least one muon inside each jet with $P_t^\mu \geq 5$ GeV in the rapidity region $-1.1 \leq \eta^\mu \leq 1.1$. 1000 events were generated and reconstructed in the barrel part at each energy point.

The results are obtained using the standard CMS reconstruction procedure (data card 'MUON' 2 and 'TRAK' 3) existing in the CMSIM version 115.

Pattern recognition in the muon stations is done by building track segments from the reconstructed hits separately in the (r, ϕ) and (r, z) planes; $(r\phi, rz)$ track segments in the same muon station and in the same or contiguous (r, ϕ) sectors are considered to form a pair used to perform the Kalman filter. This is done starting from the outermost stations and proceeding towards the inner stations with a constrained fit to the impact point (IP) with default values of $\sigma_{x,y}^{IP} = 15 \mu m$ and $\sigma_z^{IP} = 5.3$ cm. Since the decay mean transverse length (impact parameter) of the b -quarks is about $500 \mu m$ another reconstruction was made using a constrained fit to the impact point with $\sigma_{x,y}^{IP} = 500 \mu m$ and $\sigma_z^{IP} = 5.3$ cm.

The Global Track Finder (GTF) was used for pattern recognition in the CMS inner tracker. The GTF algorithm adopted for the CMS tracker must process a large number of hits per event: typically $5 \cdot 10^8$ hits at low luminosity and ten times more at high luminosity. To overcome the severe combinatorial problems, the concept of road preselection is used in the first stage of the algorithm. In the second stage a Kalman filter is used to carry out final hit selection and track fitting.

3 Track matching

Given two track segments, one in the muon system and the other in the inner tracker, one can extrapolate both segments to a common plane or point, check the difference in momentum and position and select the best combination among the candidates. The correct combination is known from the simulation procedure and it is therefore possible to calculate the efficiency of matching. We use as a matching criterion the minimal distance computed from η, ϕ and/or P_t^{rec} of the two track candidates at the outer plane (TRCI - CMSIM convention) of the inner tracker and at the impact point. Association of reconstructed tracks to GEANT ones is done on the hit basis. The reconstructed track is associated to a given GEANT particle number if more than half of the hits assigned to the track are from that particular GEANT track. If there is no such dominating track, the reconstructed track is called a "ghost". If more than one reconstructed track is matched to a given GEANT number it is called a "fake".

The η dependence of the reconstruction efficiency obtained for the barrel muon station, shown in fig. 1a) is rather uniform except for the region between the central and next-to-central rings ($|\eta| \sim 0.2$) and for $|\eta| \geq 0.9$. To avoid the influence of the η dependence of the reconstruction efficiency on the matching results the tracks with $|\eta| \geq 0.9$ are removed. The P_t reconstruction efficiency (fig. 1b)) is more than 95% for tracks with $P_t^\mu \geq 10$ GeV. In

fig. 1c) is given the "type" of reconstructed tracks in the muon stations (solid line) for which must be found the best candidate between the tracks reconstructed in the tracker (error bars). The comparison between reconstructed and generated variables: P_t , η and ϕ is given in fig. 1d) - fig. 1i) both for the barrel muon stations and for the inner tracker, for $P_t^{jet} = 100$ GeV. We find a P_t muon resolution of about 10% for the muon stations alone, and of $\leq 1\%$ for the inner tracker, in good agreement with the values given in the Muon and Tracker TDR's^[1,2].

To estimate the matching quality a χ^2 is formed from the differences between reconstructed η , ϕ and P_t in the two detectors for all reconstructed track combinations at the outer tracker plane and at the impact point:

$$\chi^2 = \sqrt{\frac{(\eta_{tr}^{rec} - \eta_{ms}^{rec})^2}{\sigma_\eta^2} + \frac{(\phi_{tr}^{rec} - \phi_{ms}^{rec})^2}{\sigma_\phi^2} + \frac{(P_{tr}^{rec} - P_{ms}^{rec})^2}{\sigma_{P_t}^2}} \quad (1)$$

Including in the χ^2 , equation (1), the contribution from P_t^{rec} in the muon stations and the tracker improves the selection of the matching tracks mainly for high transverse momenta. A minimal χ^2 of the matching tracks has been used as a matching criterion.

The P_t dependence of the matching efficiency is shown in fig. 2 for $P_t^{jet} = 50, 100$ and 200 GeV at the outer plane TRCI of the inner tracker and at the impact point with the two assumptions for the constrained fit to the impact point with $\sigma_{x,y} = 15 \mu m$ and $\sigma_{x,y} = 500 \mu m$. The degradation of the matching efficiency at higher P_t^{jet} is due to the increase of charged particle multiplicity inside jets which makes more difficult the correct association of the tracks observed in the muon stations with the track candidates in the inner tracker. The matching efficiency shows less variation when a constrained fit at the impact point is performed using $\sigma_{x,y} = 500 \mu m$.

Results obtained from the matching of muons inside the $b\bar{b}$ jets at P_t^{jet} of $50, 100$ and 200 GeV are summarized in Table 1. The "type" of the matched tracks indicates a higher purity at the impact point and at lower jet momenta. For the higher multiplicity and more collimated jets at $P_t^{jet} = 200$ GeV, the impurity in matching degrades to a $\sim 7\%$ level. Rejecting tracks with an increasing momentum threshold $\leq P_t^{cut}$, a high matching efficiency and purity of track matching can be obtained for high P_t^{jet} , but at the expense of a substantial reduction in statistics. The number of "ghost" tracks generated at reconstruction in the muon stations is negligible. The number of "fake" tracks shows some tendency to increase with jets momenta, and is at level of $1\% - 2\%$.

After performing the matching procedure we can assign to the tracks observed in the muon station the precise measurements from the tracker. The distributions of the differences between reconstructed and generated values of P_t , η and ϕ at the impact point for the matched tracks at $P_t^{jet} = 100$ GeV are given in fig. 3. These distributions are practically the same as in fig. 2, where we compared reconstructed and generated variables for the inner tracker, confirming the good quality of the matching criterion. The bottom row in fig. 3 gives the "type" of the tracks reconstructed in the muon stations and the "type" of matched tracks at the impact point.

The quality of track matching can be measured by the value of the "pull":

$$P = \frac{z_{tr} P_{tr} - z_{ms} P_{ms}}{P_{ms}^2 \sqrt{cov(1/p, 1/p)}}, \quad (2)$$

where:

z_{tr}, z_{ms} is the track charge in the tracker and the muon station;

P_{tr}, P_{ms} is the reconstructed momentum in tracker and muon station;

$cov(1/p, 1/p)$ is the covariance matrix.

A Gaussian fit to the pull shown at the bottom of fig. 3 gives $\sigma \sim 1.0$ indicating a good accuracy for the selection and matching of the tracks.

4 Summary and conclusion

The main results concerning the matching of muon tracks in $b\bar{b}$ jets between the muon stations and inner tracker are:

Using a simple minimal distance criterion between η , ϕ and P_t of independent track measurements at the impact point one can obtain a high matching efficiency with a contamination of not more than 4% for P_t^{jet} of 50 GeV and

6% for 100 GeV. For the more collimated jets with $P_t^{jet} = 200$ GeV, the impurity in matching is at a $\sim 7\%$ level.

The matching efficiency shows less variation when a constrained fit at the impact point is performed with $\sigma_{x,y} = 500 \mu m$. To further improve the matching efficiency and impurity a more sophisticated software than currently available must be used, for example, a constrained fit to the secondary $b\bar{b}$ jets vertices obtained from the inner tracker could be performed.

Rejecting tracks with an increasing momentum cut-off $\leq P_t^{cut}$, a high purity of track matching can be obtained for hard jets, but at the expense of a substantial reduction in statistics.

References

- [1] CERN/LHCC 97 - 02, G. Bayatian et al., "The Muon Project".
- [2] CERN/LHCC 98 - 06, G. Bayatian et al., "The Tracker Project".

Table 1: Track matching results.

$P_t^{jet} = 50$ GeV		TRCI		IP $\sigma_{x,y} = 15 \mu m$		IP $\sigma_{x,y} = 500 \mu m$	
P_t^{cut} (GeV)	loss of stat. (%)	efficiency (%)	impurity (%)	efficiency (%)	impurity (%)	efficiency (%)	impurity (%)
5	0	96.42	3.64 ± 0.47	96.22	4.08 ± 0.50	96.83	3.23 ± 0.45
6	2.68	96.85	2.89 ± 0.43	96.98	3.02 ± 0.48	97.06	2.81 ± 0.43
7	7.07	97.53	2.00 ± 0.37	97.73	1.86 ± 0.33	97.63	1.89 ± 0.36
8	11.98	97.97	1.60 ± 0.34	98.26	1.38 ± 0.30	98.16	1.11 ± 0.29
9	17.97	98.13	1.41 ± 0.33	98.52	1.09 ± 0.24	98.43	0.79 ± 0.25
10	24.79	98.47	0.85 ± 0.27	98.73	0.68 ± 0.23	98.46	0.60 ± 0.23
"ghost" tracks(%)		0.13 ± 0.09				0.06 ± 0.06	
"fake" tracks(%)		1.47 ± 0.30				1.45 ± 0.39	
$P_t^{jet} = 100$ GeV		TRCI		IP $\sigma_{x,y} = 15 \mu m$		IP $\sigma_{x,y} = 500 \mu m$	
P_t^{cut} (GeV)	loss of stat. (%)	efficiency (%)	impurity (%)	efficiency (%)	impurity (%)	efficiency (%)	impurity (%)
5	0	93.57	6.55 ± 0.61	94.40	6.24 ± 0.62	94.87	5.89 ± 0.59
6	2.22	93.93	6.13 ± 0.60	95.18	5.24 ± 0.56	95.61	5.05 ± 0.55
7	4.32	94.38	5.68 ± 0.59	95.66	4.71 ± 0.58	96.43	4.13 ± 0.51
8	6.49	94.78	5.28 ± 0.57	96.16	4.16 ± 0.54	96.94	3.44 ± 0.47
9	9.57	95.15	4.85 ± 0.56	96.17	3.96 ± 0.56	97.12	3.15 ± 0.46
10	13.03	95.66	4.27 ± 0.54	96.73	3.27 ± 0.48	97.30	2.84 ± 0.44
15	26.03	97.39	2.36 ± 0.44	98.06	1.77 ± 0.33	98.83	1.17 ± 0.31
"ghost" tracks(%)		0.08 ± 0.07				0.10 ± 0.08	
"fake" tracks(%)		1.78 ± 0.41				1.36 ± 0.38	
$P_t^{jet} = 200$ GeV		TRCI		IP $\sigma_{x,y} = 15 \mu m$		IP $\sigma_{x,y} = 500 \mu m$	
P_t^{cut} (GeV)	loss of stat. (%)	efficiency (%)	impurity (%)	efficiency (%)	impurity (%)	efficiency (%)	impurity (%)
5	0	90.17	9.99 ± 0.74	92.55	8.07 ± 0.67	94.12	6.90 ± 0.62
6	0.60	90.60	9.51 ± 0.72	93.00	7.51 ± 0.69	94.33	6.59 ± 0.61
7	1.62	91.18	8.94 ± 0.71	93.42	6.98 ± 0.66	94.70	6.12 ± 0.60
8	3.25	91.72	8.40 ± 0.69	93.69	6.72 ± 0.67	95.00	5.48 ± 0.57
9	5.05	91.94	8.17 ± 0.69	94.15	6.14 ± 0.68	95.24	5.07 ± 0.56
10	6.80	92.24	7.88 ± 0.68	94.56	5.75 ± 0.52	95.21	5.04 ± 0.56
15	17.63	93.69	6.38 ± 0.65	95.98	4.23 ± 0.53	96.44	3.70 ± 0.51
20	23.95	94.86	5.07 ± 0.62	96.75	3.25 ± 0.41	97.50	2.65 ± 0.46
"ghost" tracks(%)		0.18 ± 0.10				0.18 ± 0.10	
"fake" tracks(%)		1.99 ± 0.34				2.11 ± 0.35	

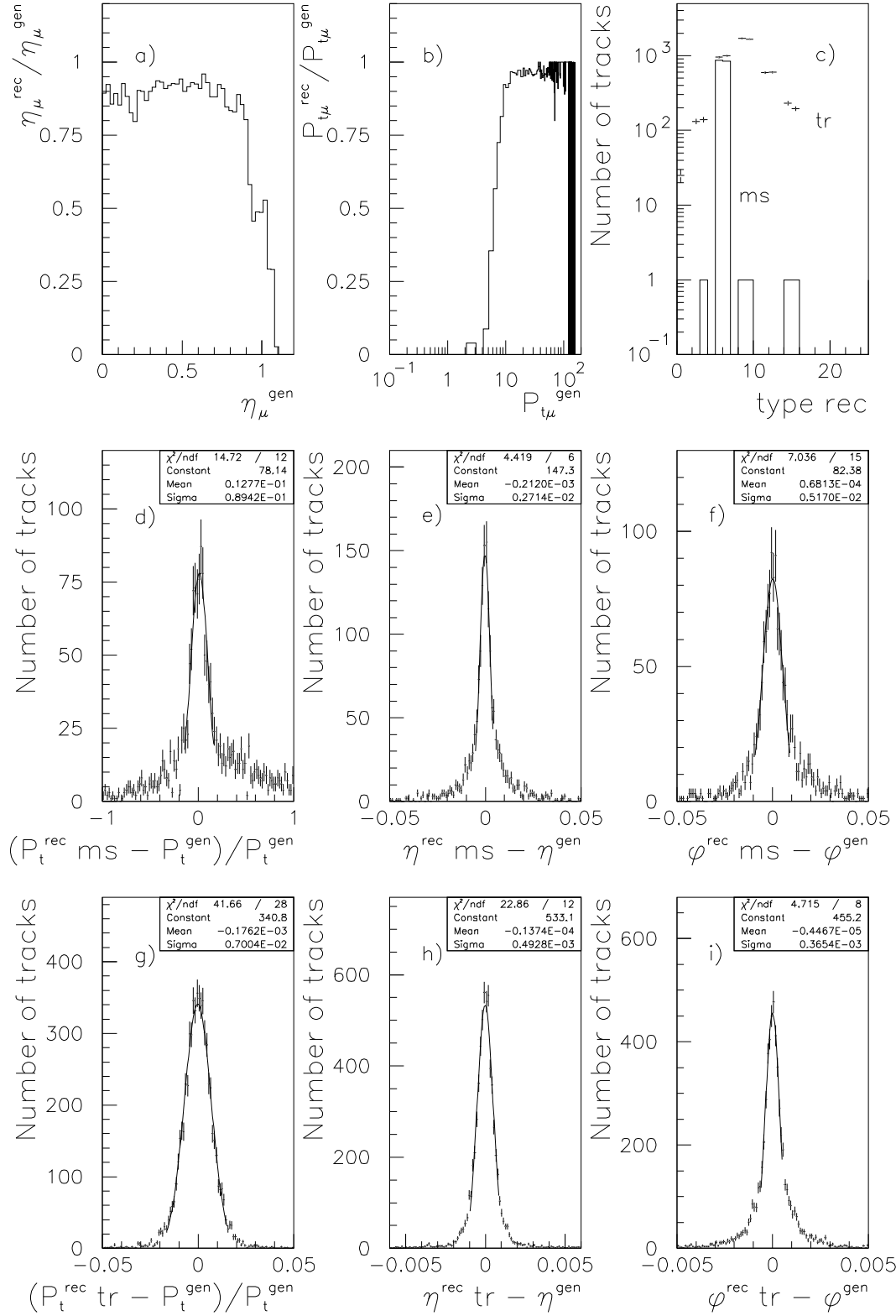


Figure 1: η (a) and P_t (b) dependence of the reconstructed efficiency, "type" of reconstructed tracks (c) in the muon stations (solid line) and in the tracker (error bars) and comparison between reconstructed and generated variables P_t , η and ϕ in the barrel muon station (d - f) and in the inner tracker (g - i) for $P_t^{jet} = 100$ GeV.

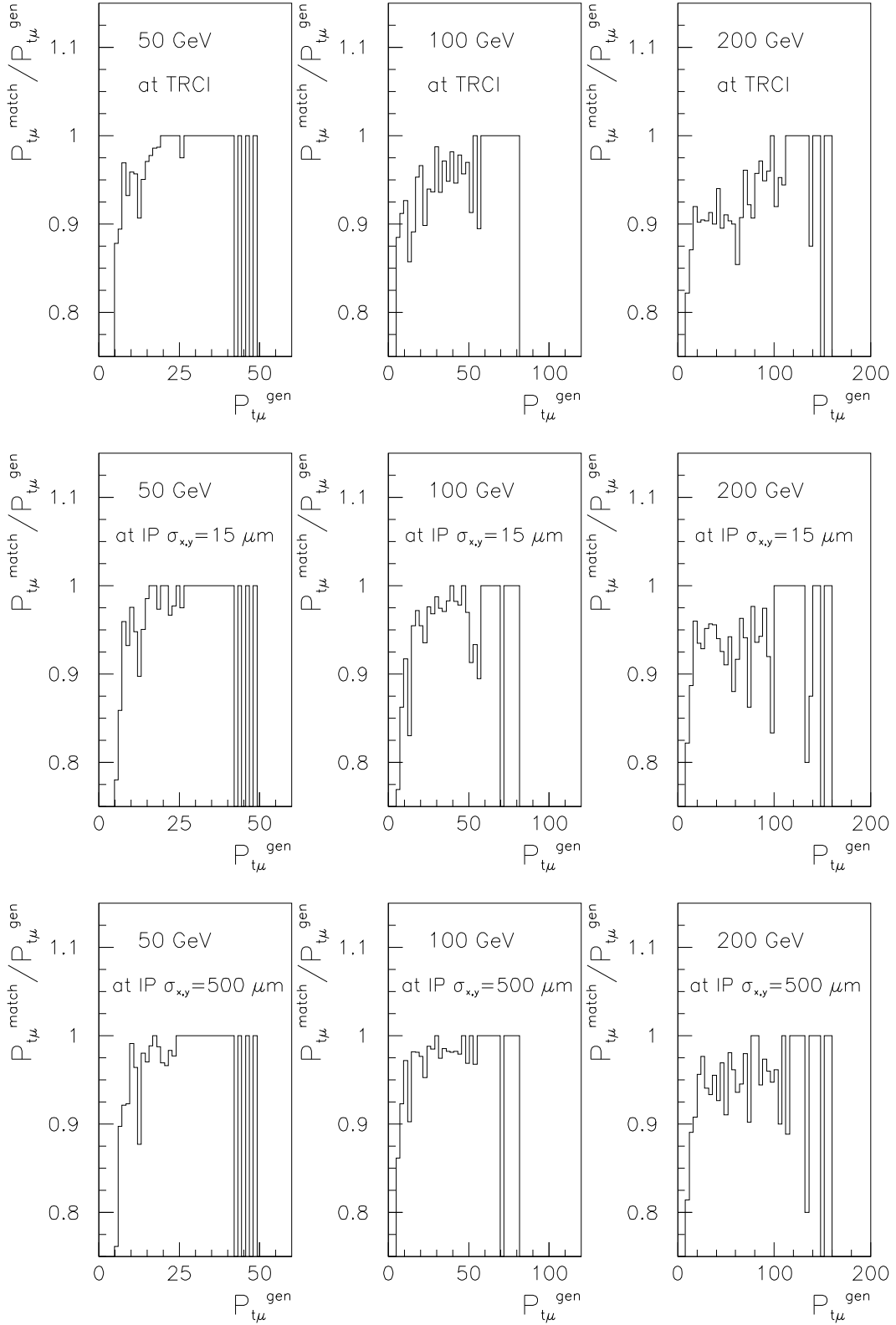


Figure 2: P_t dependence of the matching efficiency for $P_t^{jet} = 50, 100$ and 200 GeV at the outer plane TRCI of the inner tracker and at the impact point with two assumptions for the constrained fit to the impact point with $\sigma_{x,y} = 15 \mu m$ and $\sigma_{x,y} = 500 \mu m$ respectively.

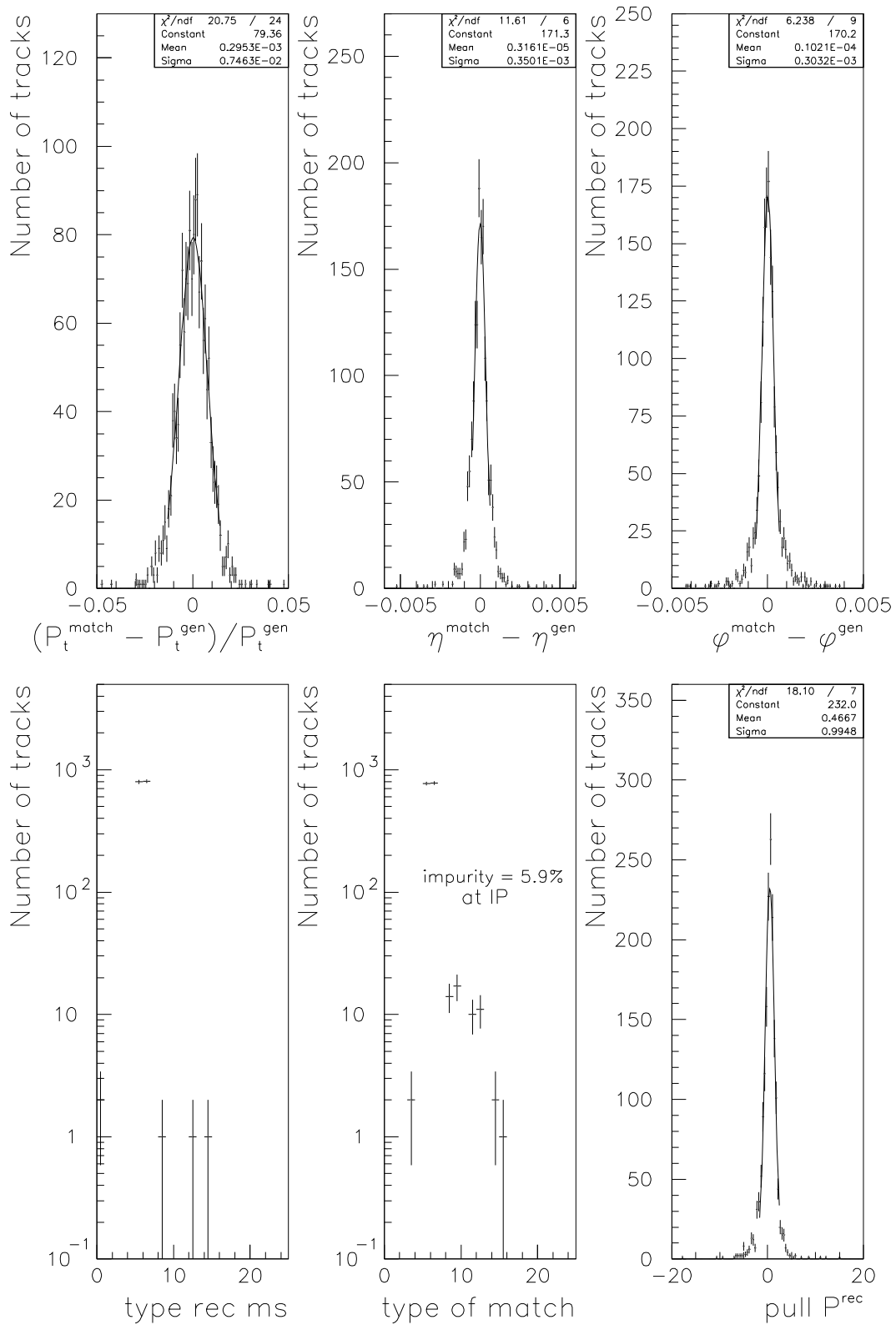


Figure 3: Comparison of reconstructed and generated values of P_t , η and ϕ , "type" and "pull" for matched tracks at impact point for $P_t^{\text{jet}} = 100$ GeV.